Ann. Rev. Astron. Astrophys. 1986. 24 : 577–611

STAR COUNTS AND GALACTIC STRUCTURE

John N. Bahcall

Institute for Advanced Study, Princeton, New Jersey 08540

1. INTRODUCTION

Star counts is a subject whose time has passed and come again. The reasons for its resuscitation are the use of automatic measuring devices, a change of theoretical tactics, and the development of a detailed model that can be used with modern computers. All three of these factors developed at approximately the same time and have led to a renewal of interest in galactic star counts. In this section, we explore some of the reasons why counting stars has again become a respectable and profitable way to learn about galactic structure. But first we must briefly recall the classical research on this subject in order to see what has changed.

The pioneering work on star counts is described by Bok (1937) in a unique book that is as charming as it is informative. The early developers of this subject, a group that includes Kapteyn (1922), Seares and van Rhijn (see, e.g., Seares 1924, Seares et al. 1925), Bok [see references in Bok (1937) and Bok & Basinski (1964)], and Oort (1938), used star counts in an effort to determine the geometrical structure of the Galaxy and to measure the amount of obscuration that is present. They tried to invert the fundamental equation of stellar statistics (see the introduction to Section 2) in order to infer the shapes and parameters of the different stellar populations. This effort had limited success because of the pervasive and patchy nature of obscuration (which was Kapteyn's undoing) and because of the limited amount of well-calibrated data. The inversion of the integral equation for the projected number of stars on the sky is also an unstable mathematical procedure that can produce unreliable results when the number of stars is small and the photometric accuracy is not high. A modern account of this procedure, with a review of the earlier work, is contained in Mihalas & Binney (1981, p. 277). The classical procedures have been used most recently by Becker (1980) and by Gilmore & Reid (1983).

0066–4146/86/0915–0577$02.00

Important collections of star counts and colors are contained in the older work of Seares et al. (1925) and in the catalogs of the Basel survey (Becker 1965, Becker & Steppe 1977, Fenkart 1967, 1968, 1969, Fenkart & Wagner 1975, Schaltenbrand 1974, Fenkart & Schaltenbrand 1977, Yilmaz 1977). These data contain valuable information about the Galaxy and its stellar content that has only been partially extracted.

The observational situation has changed dramatically in recent years. Modern and (in most cases) more accurate data on star counts are being published with increasing frequency in highly readable papers (see, e.g., Weistrop 1972, Kron 1978, 1980, Peterson et al. 1979, Chiu 1980, Jarvis & Tyson 1981, Koo & Kron 1982, Morton & Tritton 1982, Reid & Gilmore 1982, Gilmore & Reid 1983, McLaughlin 1983, Ratnatunga 1983, Sandage 1983, Friel & Cudworth 1986, Infante 1986, Rodgers et al. 1986, and the many references contained in these important papers).

One could more than double the available published high-quality data for star-count analysis, acquired over the past 60 years of research, by devoting one month of continuous scanning with one of the modern devices for automatically measuring Schmidt plates (like the Cosmos machine at the ROE or the APM in Cambridge) or by making deep dedicated surveys with charge-coupled devices. As a by-product, the guide-star selection system for the *Hubble Space Telescope* (Lasker 1985) and the surveys of the cameras aboard the HST observatory will result in a great increase in our knowledge of well-calibrated star distributions.

Now that many good data are available and much more are on the horizon, what can one do with them?

The problems with the previous methods of analyzing star counts can be avoided (Bahcall & Soneira 1980, Pritchet 1983) by *assuming* that the geometrical distribution of stars in the Galaxy is similar to that observed in other galaxies of the same Hubble type and by only comparing the model with observations in regions in which the obscuration is known to be small. This change of tactics uses star counts to determine parameters in functions whose overall shape is assumed known and avoids obscuration rather than trying to determine it.

We also use a different approach to the theoretical analysis of star counts. We do *not* invert the equation of stellar statistics. Instead, we assume a model, calculate the expected results in terms of the observational parameters (numbers per unit magnitude per color bin), and iterate the model with the aid of a computer until the calculated results agree with the observations to within the estimated errors. This procedure does not lead to a unique model, since small components with special properties can always be added without destroying significantly the agreement between

calculation and observation. But it does determine relatively well some of the basic characteristics of the Galaxy.

In summary, with the tactics described above, we can determine only relatively few things, but the things we do determine are relatively well established.

I shall devote most of this review discussing what can be learned about the Galaxy and its stellar content from the simplest version of a "copycat" Galaxy model (one whose shape is chosen by analogy with other galaxies) with a Population I disk and a Population II spheroid. Only at the end of this review will I discuss extensions and improvements of this model. We shall see next that this simple (and conventional) model gives a surprisingly accurate description of the observed distributions in brightness and color of hundreds of thousands of stars in different directions, in different magnitude ranges, and in different broadband colors.

Figure 1 shows the 17 fields in which the model of Bahcall & Soneira

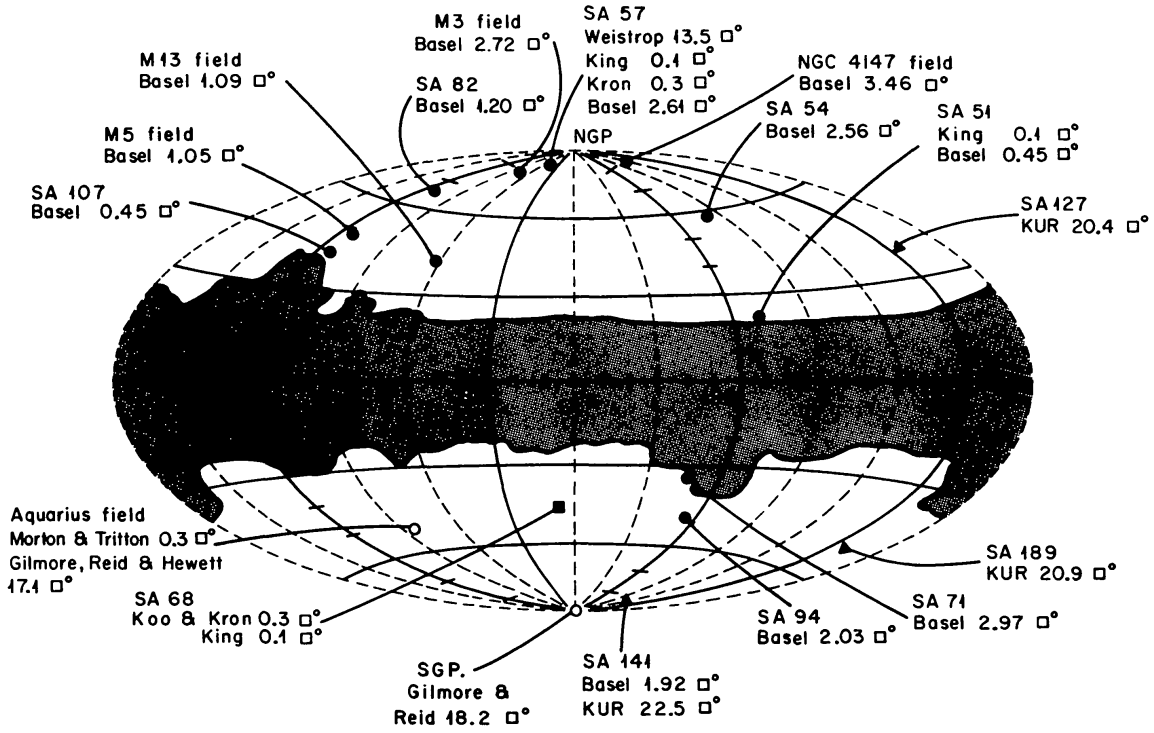

Figure 1 Fields in which the Bahcall-Soneira Galaxy model has been tested. The standard Galaxy model (Paper II) fits well the published observations in all of the 17 fields shown. The different observing groups that have studied each field are listed below the label for that field. References to the original observational papers are given in the main text and in Bahcall et al. (1985), from which this figure is taken. The zone of avoidance that is shown by the shaded area has galactic latitude $b < 20°$ or $E(B-V) > 0.1$ mag (according to Burstein & Heiles 1982).

(1980, 1984) (hereinafter Papers I and II, respectively) has been tested. In all cases, the agreement with observations is satisfactory. [Friel & Cudworth (1986) and Infante (1986) have studied two new fields in which the model also fits well.] The model predicts the characteristic distribution of stars in apparent magnitude and in color over a wide range in apparent magnitudes. (The extreme range over which the observational comparisons have been made is $m_V = 5$–22 mag.) The best way to get à feel for the basic validity of the model is to see how the predicted distributions change with magnitude and color as one calculates the results for different directions in the sky.

Figures 2–11 show a number of different directions, magnitude ranges, and colors in which the observed and predicted star distributions are compared. Both the *shapes* of the distributions and the *absolute numbers*

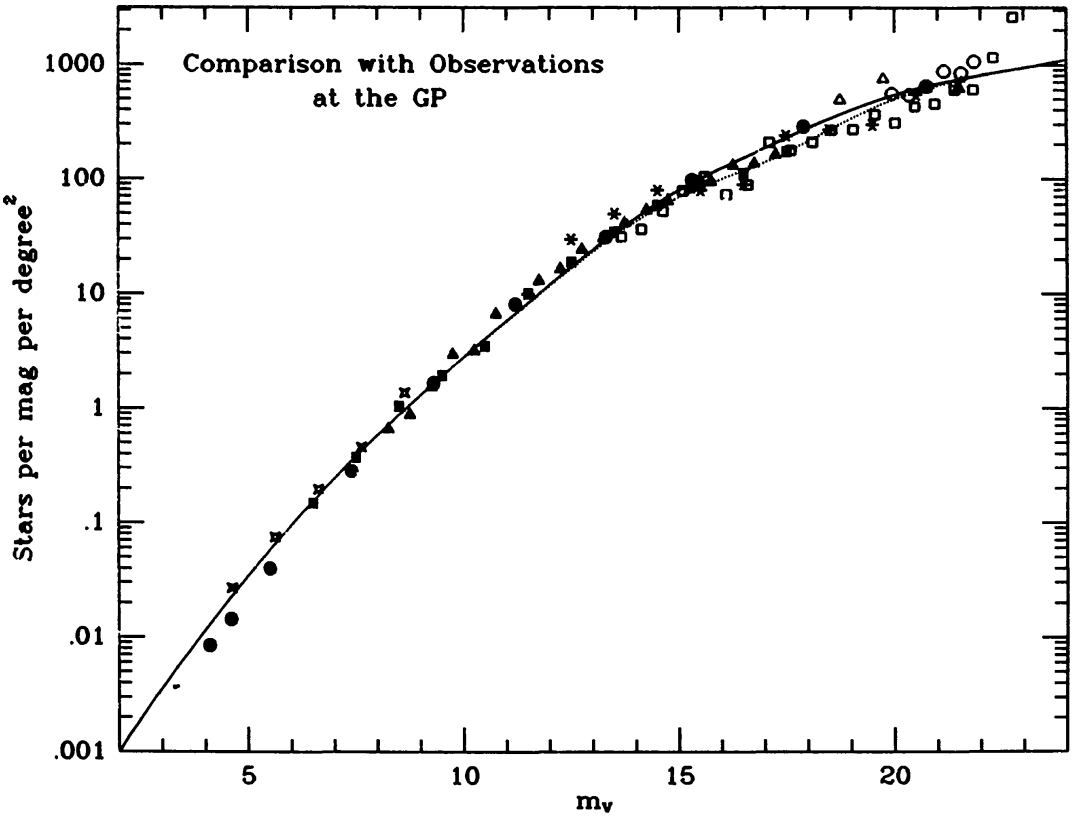

Figure 2 The north galactic pole. Differential star counts per magnitude per square degree for the galactic pole. The solid curve is predicted by the standard model. Data from Seares et al. (1925) as reduced to the visual band in Paper I are plotted as filled circles; data from Weistrop (1972) with Faber et al. (1976) corrections as filled squares; data from McLaughlin (1983) as open crosses; data from Reid & Gilmore (1983) as filled triangles; data from King (Chiu 1980) as asterisks; data from Jarvis & Tyson (1981) as open squares; data from Peterson et al. (1979) as open triangles; and data from Kron (1978, 1980) as open circles. This figure is taken from Paper II.

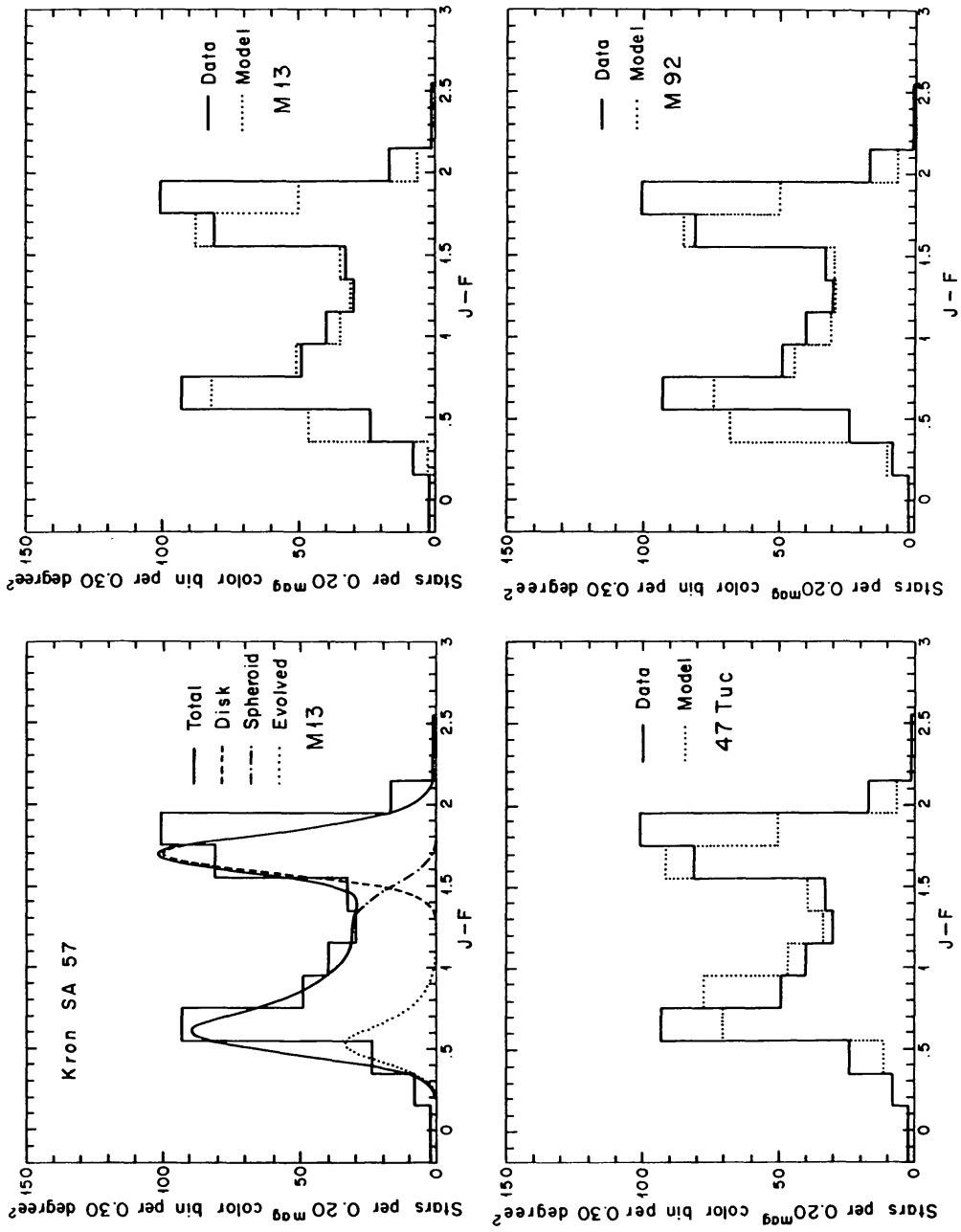

Figure 3 Comparison of the calculated color distributions with Kron's observations of faint stars in SA 57. Kron's sample contains stars between $(J+F)/2 = 19.95$ mag and $(J+F)/2 = 21.75$ mag. The ordinate gives, both for the observations and the calculations, the number of stars in 0.3 degree^2. The calculated colors have been convolved with a color dispersion having a standard deviation of 0.1 mag in $J-F$. The color-magnitude diagram of M13 was used for the spheroid in calculating the distributions shown in the top two diagrams. Color-magnitude diagrams of 47 Tuc and M92 were assumed for the spheroid in the calculations shown in the bottom two diagrams. The contribution of subgiants and giants is denoted by the curve labeled "evolved." This figure is taken from Paper II.

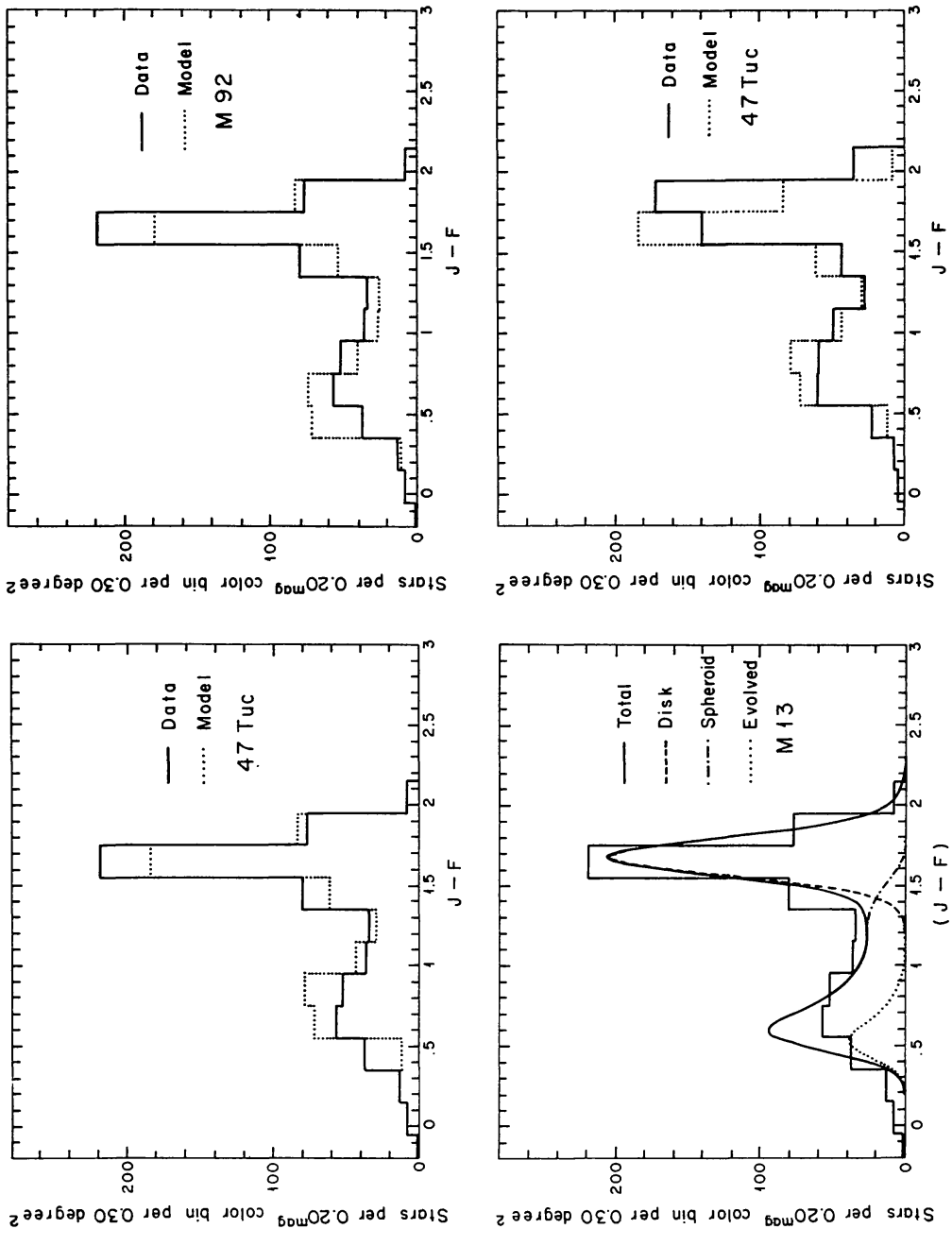

Figure 4 Comparison with color distributions of faint stars in SA 68 obtained by Koo & Kron. The top two diagrams compare the color histogram of faint stars observed by Koo & Kron (1982) with the distribution calculated using the Bahcall-Soneira Galaxy model and a color-magnitude diagram like 47 Tuc for the spheroid (upper left) or a spheroid color-magnitude diagram like M92 (upper right). The figure shows the breakdown into individual components; the spheroid was assumed to have a color-magnitude diagram like M13 for this illustration. The contribution of subgiants and giants is labeled "evolved." The bottom right diagram compares the original Kron (1978, 1980) data with the color-distribution obtained using a spheroid color-magnitude diagram like 47 Tuc. This figure is taken from Paper II.

of the stars are important. For each area, I show the number of stars that are observed and predicted. *Both the predicted star counts and the observed distributions change drastically with the color range, the magnitude range, and the direction considered, but they are always in a reasonable agreement.* I think anyone who studies these figures [and the many other comparisons in Paper I and II and Bahcall et al. (1985)] will be convinced that the two-component model is a reasonable first approximation to the observed stellar content of the Galaxy.

Now that we have seen that there are many data and that a simple model gives an acceptable description of the observations, we need to ask, What is this model and what is it good for? In Section 2 I define the model in

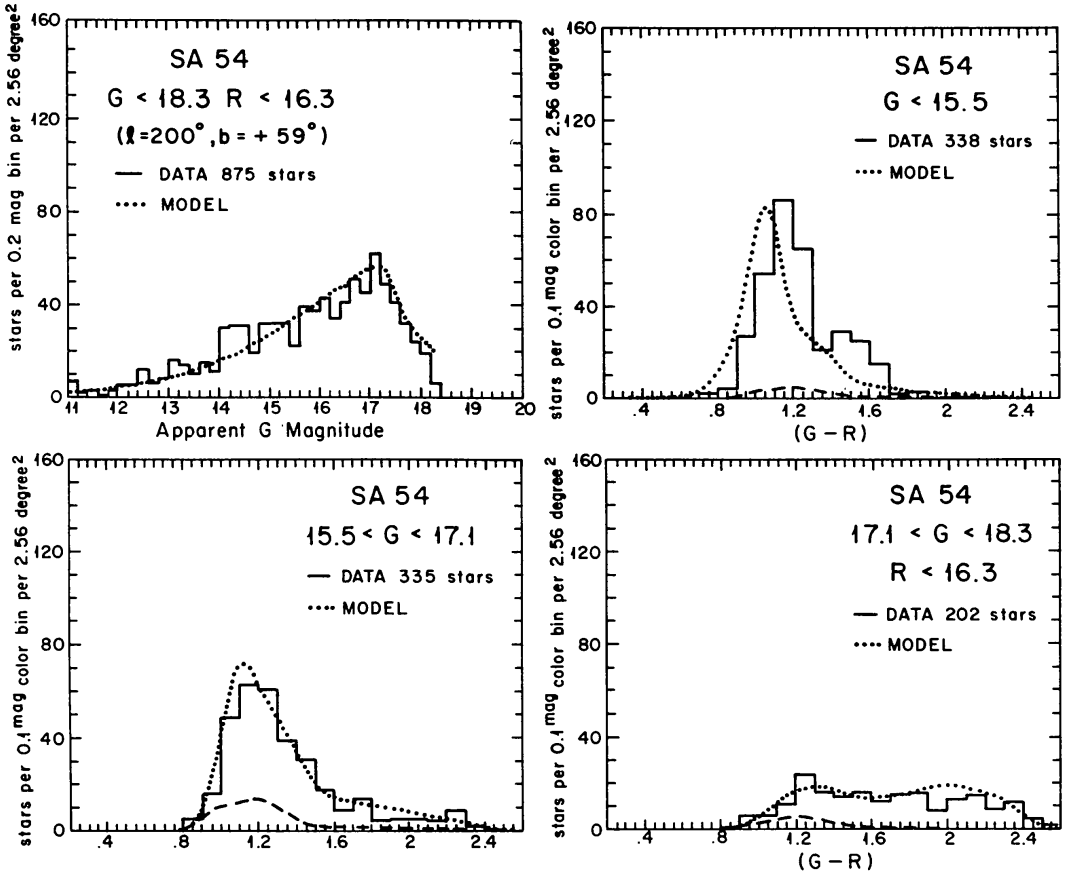

Figure 5 Basel G and R data for field SA 54. The upper left diagram compares the apparent distribution in G for the total sample selected with both R and G magnitude limits. The R magnitude limit affects only the faintest apparent magnitude range; the two other apparent G magnitude ranges were selected to have about equal numbers of stars. The other three diagrams compare the observed $(G-R)$ color distribution (histogram) with the distributions calculated from the Bahcall-Soneira Galaxy model (dotted line) for three apparent magnitude ranges in SA 54. The contribution of the spheroid to the counts was calculated by assuming a 47 Tuc color-magnitude diagram and is shown by the dashed line. A reddening of $E(B-V) = 0.0$ mag was used in the model. This figure is taken from Bahcall et al. (1985).

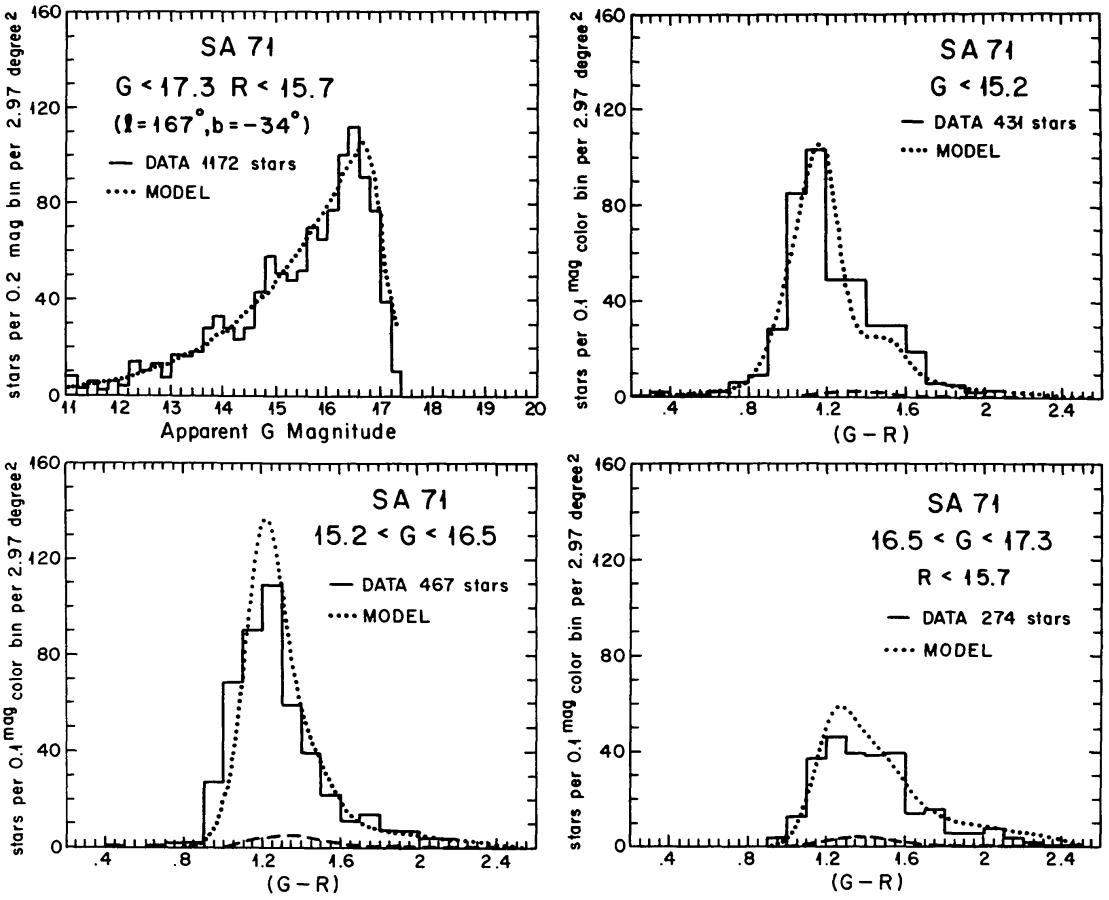

Figure 6 Basel *G* and *R* data for field near SA 71. Diagrams were constucted in the same way as those in Figure 5.

detail, and in Section 3 I discuss its applications. In Section 4 I answer the question, what next?

I do not expect that anyone will read this paper in the order in which it is written. Most readers will want to begin by glancing through Section 3 to find out which of the 11 applications discussed there are relevant for their interests. Typical readers may then wish to review Section 4.2 to see what other questions can be answered by future observations. Only if they find something especially relevant in the applications or future questions sections will most readers find it worthwhile to read the detailed description of the model (in Section 2) or the discussion of future improvements (Section 4.1).

2. THE GALAXY MODEL

Galaxy models can be constructed with more or less complexity (cf., e.g., Bahcall & Soneira 1980, Buser & Kaeser 1983, 1985, Pritchet 1983, Gil-

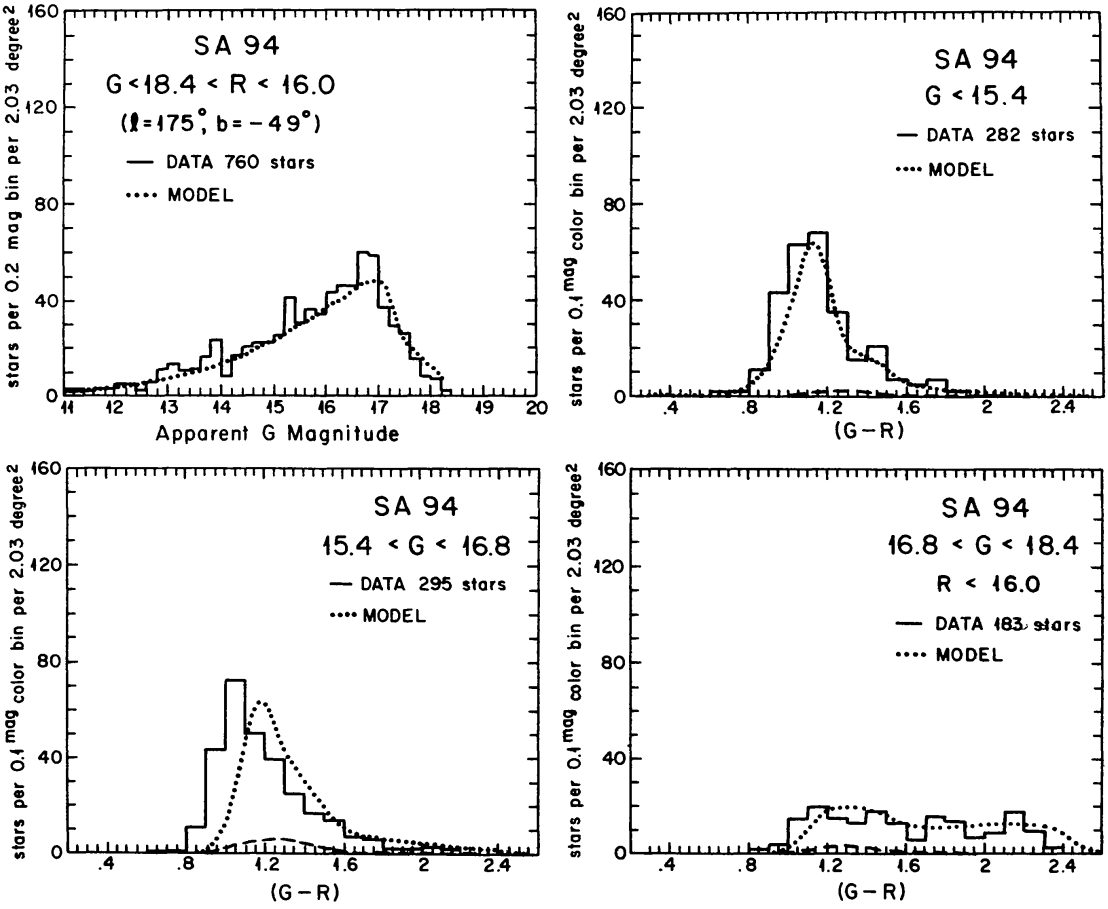

Figure 7 Basel G and R data for field near SA 94. Diagrams were constructed in the same way as those in Figure 5, except that $E(B-V) = 0.02$ mag was used in the model.

more 1984, Creze & Robin 1986). However, in my opinion, the tactics of avoiding obscuration and of comparing the calculated star distributions in the space of observed parameters are more important for future developments than are the current details in any particular model. For specificity, I concentrate in this paper on illustrating how these tactics can be applied by making use of the model that is usually referred to in the literature as the Bahcall-Soneira (or B&S) model.

The B&S model is realized in the form of an Export Code that has been circulated to different researchers. The basic components are embodied in the code as subroutines so that they can be changed independently. Once appropriate observations are available and a unique improvement has been identified, the relevant subroutine of the code can be modified. The model is not a static conception. Instead, it is a tool for learning about the Galaxy. Details should be added as we learn more about the stellar content of the Galaxy.

Most of the applications that are described in this review refer to a two-

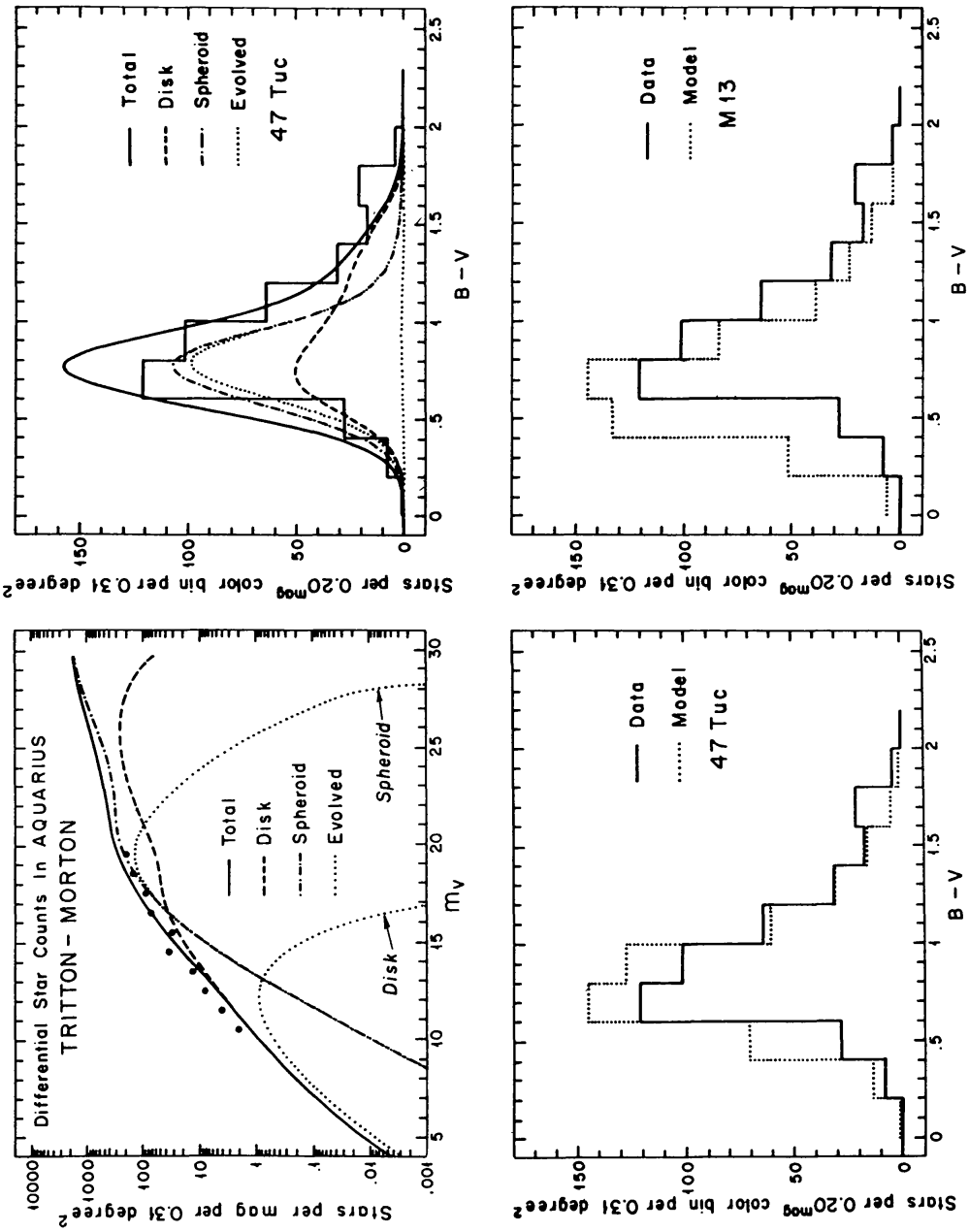

Figure 8 Comparison with the Morton-Tritton star counts and color distributions in Aquarius. The total number of observed stars is 399. The upper left diagram compares the observed and calculated differential star counts. The other three diagrams compare the observed and calculated color distributions to $V \leq 19$. A spheroid color-magnitude diagram like that of 47 Tuc was assumed in the calculations that are described by the upper right and lower left diagrams; a color-magnitude diagram like that of M13 was used for the bottom right diagram. Following Morton & Tritton (1982), we have assumed a color dispersion in $B-V$ of 0.15 mag. This figure is taken from Paper II.

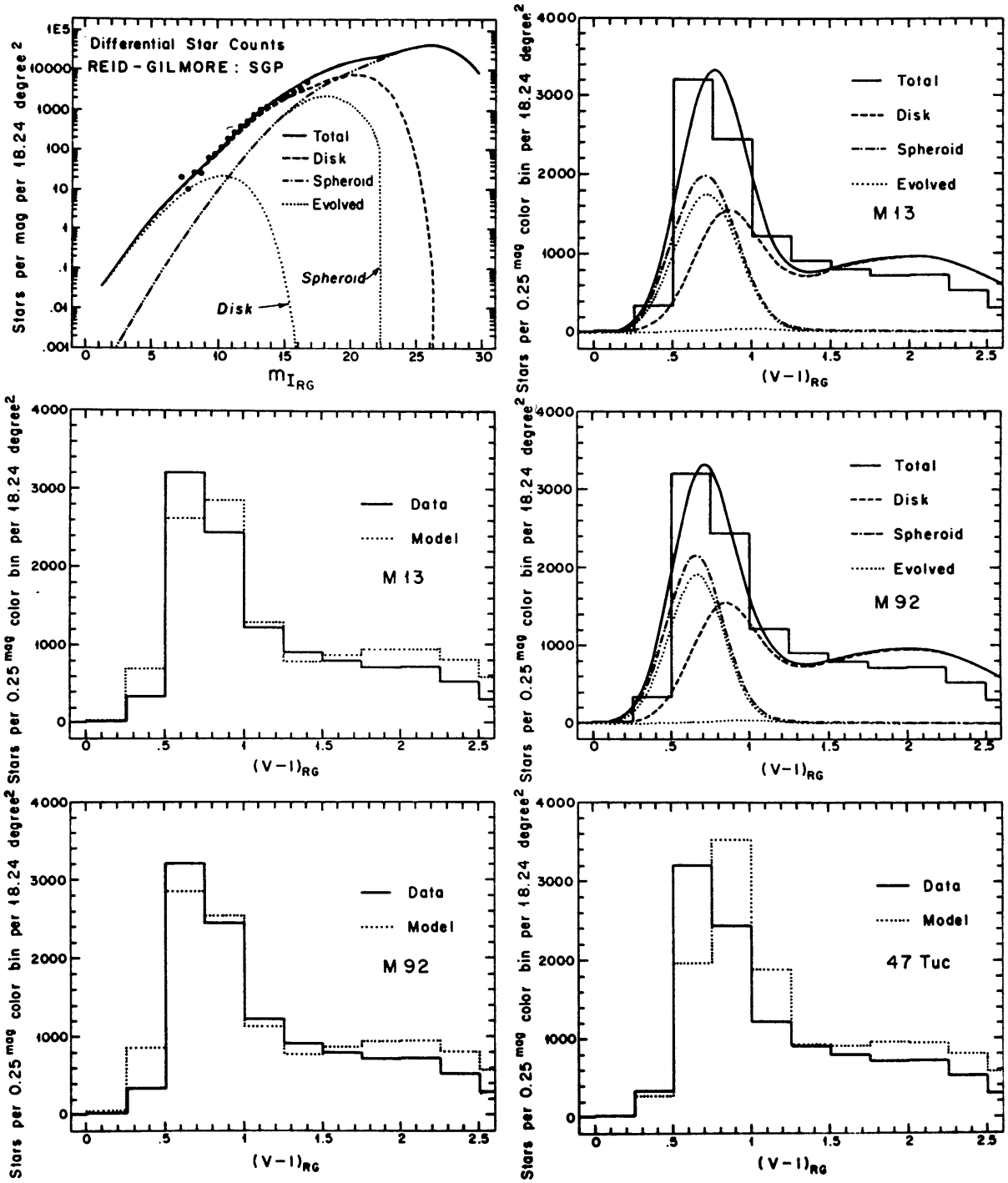

Figure 9 Comparison with the Reid-Gilmore survey of the south galactic pole. The observations in V and I by Reid & Gilmore (1982) are compared with the calculated distributions. This figure is taken from Paper II.

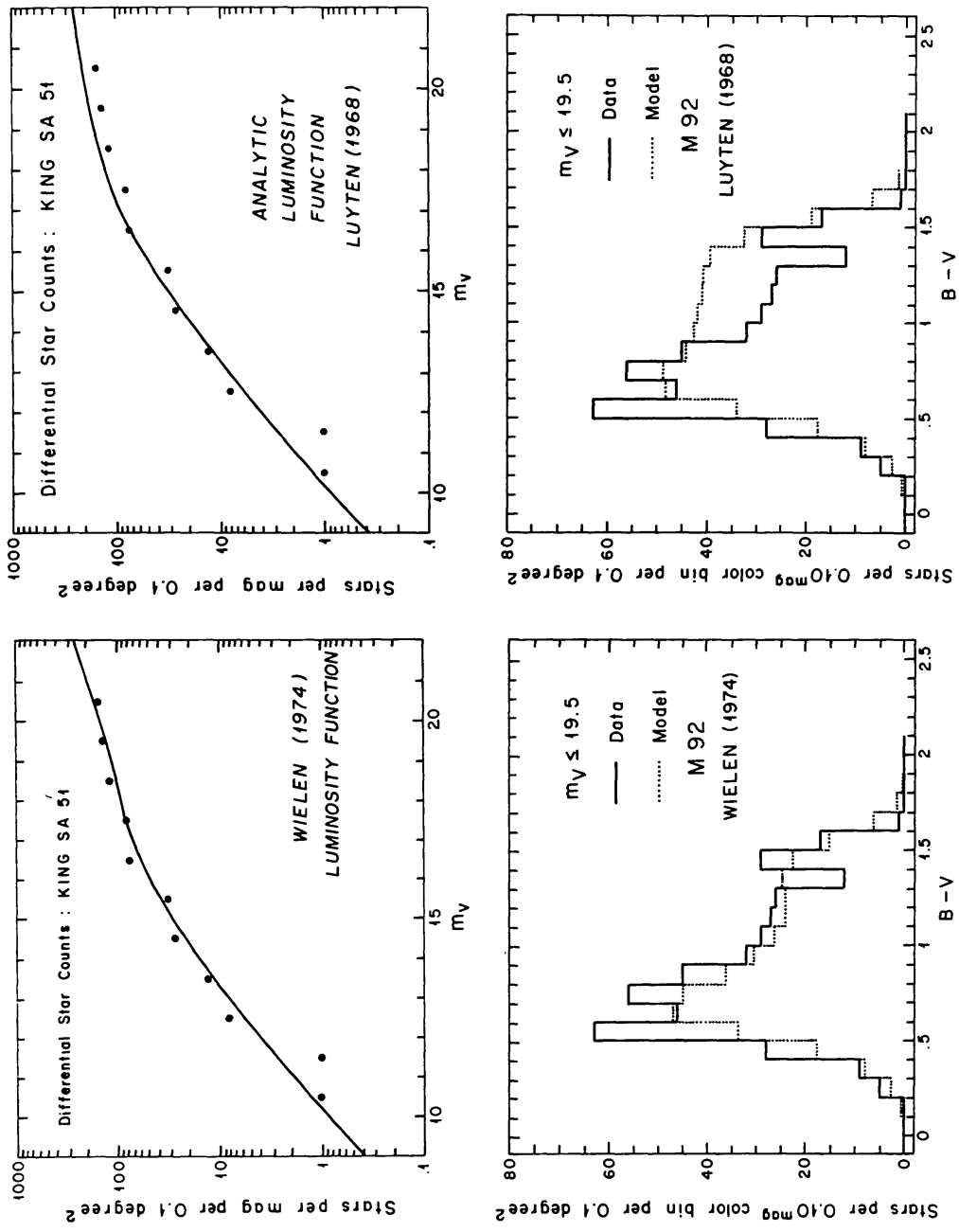

Figure 10 Wielen versus Luyten luminosity functions for King's data in SA 51. The upper two diagrams compare the observed differential star counts with those calculated using a Wielen (1974) or a Luyten (1968) luminosity function. The bottom two diagrams make a similar comparison for the color distribution. The observations indicate that the Wielen luminosity function is preferred. This figure is taken from Paper II.

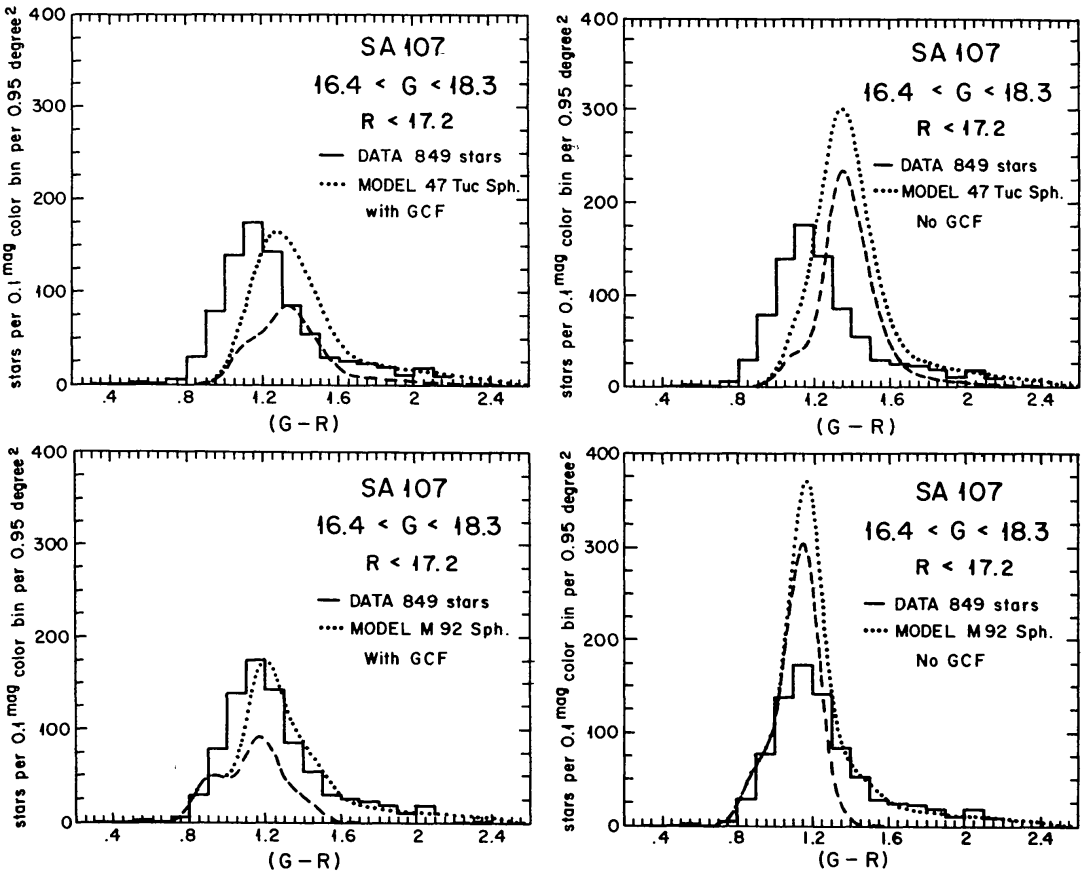

Figure 11 The globular cluster feature (GCF) is required to fit the observed star distribution in SA 107. The observed $(G-R)$ color distribution (histogram) is compared to the predictions of the model (dotted line) for SA 107. The estimated contribution of the spheroid to the counts is shown by the dashed line. In constructing the upper left diagram, the color-magnitude diagram of 47 Tuc was used for the spheroid. The GCF was included in the spheroid luminosity function. The upper right diagram was calculated in the same way except that the GCF was omitted. The bottom two diagrams are the same as those in Figure 12, except that the color-magnitude diagram of M92 was used for the spheroid. In all the models, $E(B-V) = 0.09$ was assumed. This figure is based upon data from the Basel survey and is taken from Bahcall et al. (1985).

component (copycat) model containing only a Population I disk and a Population II spheroid. Other components are presumably present, and I discuss briefly the effects of adding a massive unseen halo, a galactic bulge, and a thick disk. Of course, there is much more in the Galaxy than is in any theoretical model. The question I address here is how well can a simple model account for the major observed stellar components.

We adopt as a first approximation an additional simplification. We assume that the characteristics of the disk and spheroid (e.g. luminosity functions or age) are *independent of position* in the Galaxy. We expect that departures from this approximation will be observed in general star counts,

e.g. for young disk stars and for the metallicity of the spheroid field stars. However, it is much easier to state an approximation like the one given above, which we believe to be wrong at some level, than it is to *prove* conclusively that the approximation is in conflict with observations.

With the above assumptions, the surface number density of stars, $A_i(m_1, m_2, l, b)$ that have apparent magnitudes in the interval $m_1 \leq m \leq m_2$ in the direction (l, b) per projected area on the sky $d\Omega$ can be calculated for each stellar component i by using the specified luminosity functions and number densities. The surface density of stars may be expressed in the form

$$A_i(m_1, m_2, l, b)\, d\Omega = \int_{m_1}^{m_2} dm' \int_0^{\infty} dR\, R^2 \rho_i(\mathbf{r}, M)\phi_i(M)\, d\Omega, \qquad 1.$$

where the absolute magnitude M satisfies $M = m' - 5 \log R - \Theta(R) + 5$, the vertical height above the plane is $z = R \sin b$, the distance in the plane is $x = [r_0^2 + R^2 \cos^2 b - 2Rr_0 \cos b \cos l]^{1/2}$, and the galactocentric distance is $r = [x^2 + z^2]^{1/2}$. The total number of stars is, in the simplest approximation, the sum of the disk and spheroid distributions ($A_T = A_d + A_s$). Here Θ is the total galactic obscuration in the direction (l, b) out to a distance R from the Sun. The star densities ρ and luminosity functions ϕ are defined below. The model does not distinguish between northern and southern galactic latitudes, i.e. $b = |b^{II}|$.

The integral equation given above for the total star counts A_T is often known as the fundamental equation of stellar statistics. The classical technique for studying star counts (see Bok 1937, Mihalas & Binney 1981) is to invert this equation to solve for the density, the luminosity function, and the obscuration. Instead, the Galaxy model calculates the integral in terms of observed parameters (e.g. apparent magnitudes, colors) for both the disk (A_d) and the spheroid (A_s) star counts.

Three different expressions are available in the model for the galactic obscuration $\Theta(R)$ [no obscuration, the cosecant model, and the Sandage (1972) modified cosecant law]. One can also insert directly into the model the Burstein & Heiles (1982) values for a particular direction. If the answer one obtains depends significantly upon which reddening or obscuration law is used, then the results are unreliable and cannot be trusted either as a test of the model or as indicators of galactic structure.

2.1 *The Mass Distribution*

The basic assumption made in constructing the Galaxy model is that the geometric shape of the stellar components is the same as has been established for other galaxies of the same Hubble type (Sb to Sc). The stellar

density laws used for the disk and spheroid in our standard model of the Galaxy are given in Table 1. We use an exponential disk in the plane for the Population I stars and a de Vaucouleurs (1959) law for the Population II spheroid stars. We also assume that the density of each kind of disk star falls off exponentially perpendicular to the plane because self-consistent solutions of the Poisson and Vlasow equations are well described by exponentials in the region of interest [see Figure 8 of Bahcall (1984) and the related discussion].

We have tested (see Paper I) the sensitivity of our inferences to the assumed geometry by performing a series of calculations with different model shapes and parameters. We also investigated exponential disks with holes around the galactic center and spheroid mass distributions that are described by a Hubble (1930) law instead of a de Vaucouleurs law. Plausible variations in geometry did not produce differences in the predicted counts that were large enough to be detected easily in the available data (cf. Buser & Kaeser 1985).

The next step in extending the Galaxy model will be to add a galactic bulge. The mass distribution for this component is also shown in Table 1.

Table 1 The assumed stellar distributions

Component	Distribution
Disk	$n_D = n_D(R_0)\exp[-z/H(M_V)]\exp[-(x-R_0)/h]$
Spheroid	$n_{sph} = n_{sph}(R_0)(R/R_0)^{-7/8}\left\{\exp\left[-10.093(R/R_0)^{1/4}+10.093\right]\right\}$
	$\times 125(R/R_0)^{-6/8}\left\{\exp\left[-10.093(R/R_0)^{1/4}+10.093\right]\right\}, \quad R < 0.03R_0$
	$\times\left[1-0.08669/(R/R_0)^{1/4}\right], \quad R \geq 0.03R_0$
Central Bulge	$\rho = \rho_c\alpha^{-1.8}\exp(-R/1\ kpc)^3$
	$\alpha^2 = (x^2+6.25z^2)$ $(x,z$ in $pc)$
Halo	$\rho = \rho_H(R_\odot)\left(\frac{a^{1.2}+R_0^{1.2}}{a^{1.2}+R^{1.2}}\right)\times\begin{cases}1, & R \leq R_c\\ (R/R_c)^{1.5}, & R > R_c\end{cases}$
Normalization	$n_D(R_0) = 0.13\ pc^{-3}$, $n_{sph} = 0.00026\ pc^{-3}$, for $M_V \leq 16.5$ mag
	$\rho_c = 7.6\times 10^5 M_\odot pc^{-3}$ and $\rho_{Halo}(R_0) = 0.009 M_\odot pc^{-3}$.

Note: Here z is the distance perpendicular to the plane, x is the galactocentric distance in the plane, and h is the disk scale length. Galactocentric distance $R = (x^2+z^2/\kappa^2)^{1/2}$, where κ is the axis ratio and $1-\kappa$ is the ellipticity. We adopt $R_0 = 8$ kpc and $h = 3.5$ kpc. This analytic form of the de Vaucouleurs law is taken from Young 1976. The fraction of disk stars that are on the main sequence is given, in the plane of the disk, by eq. (1) of Paper III.

The total masses are derived in Papers I and III: $M_{Disk} \approx 6\times 10^{10}M_\odot$, $M_{Spheroid} \approx (1-3)\times 10^9 M_\odot$, $M_{Central} \approx 1\times 10^{10}M_\odot$ and $M_{Halo}(\leq 60\ kpc) \approx 6\times 10^{11}M_\odot$.

For some applications, we have also introduced a massive halo, the fourth component in Table 1.

The mass distributions shown in Table 1 were used in computing the rotation curve of the Galaxy. The contribution to the rotation curve for each of the mass components is given for a typical theoretical rotation curve in Table 4 of Bahcall et al. 1983a (hereinafter Paper III).

The existence of a fifth component, a thick disk, has been advocated by Gilmore & Reid (1983). We shall see in Section 3 that the evidence is not yet sufficient to decide whether or not our Galaxy has a thick disk with the properties suggested by Gilmore & Reid.

2.2 *Luminosity Functions*

2.2.1 THE DISK The luminosity function used by Bahcall & Soneira (1984) for the disk stars was determined by Wielen (1974) from observations of nearby stars brighter than $M_V = 12.5$. The shape of the luminosity function is shown in Figure 12. The total number density of stars brighter than $M_V = 16.5$ in the model is 0.13 stars pc^{-3}.

For definiteness, we have assumed that the disk luminosity function is constant between absolute visual magnitudes of 12.5 and 16.5 (i.e. down

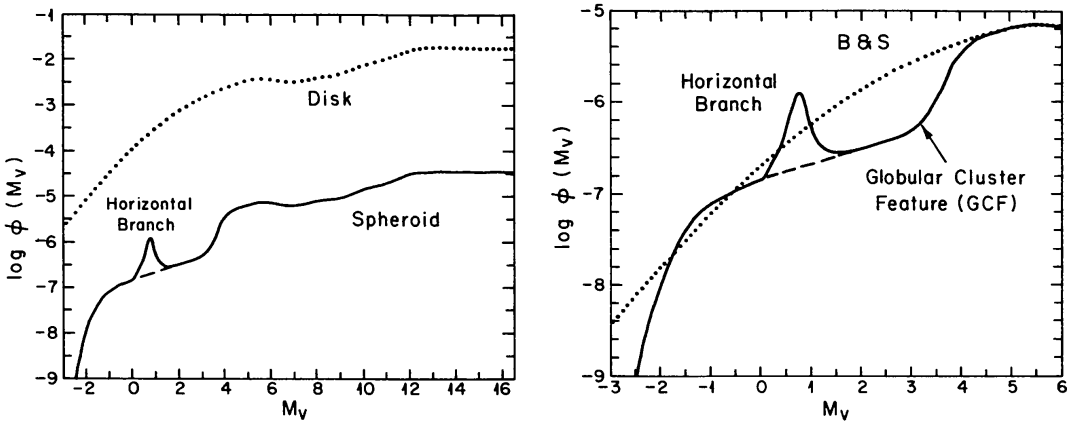

Figure 12 (*right*) The adopted disk and spheroid luminosity functions. The luminosity function for the disk is taken from Wielen (1974) for $M_V < 12.5$ and is assumed constant for $M_V > 12.5$. The spheroid luminosity function for $M_V > 4.5$ is assumed for simplicity to have the same shape as that of the disk. It is normalized to contribute 0.002 of the stars in the solar neighborhood. The spheroid luminosity function for $M_V < 4.5$ is assumed to be the same as that of the globular cluster 47 Tuc (Da Costa 1982). The two functions were joined smoothly near the turnoff at $M_V = 4.5$. The contribution from the horizontal branch (peak above the dashed line at $M_V = 0.8$) was assumed to contribute uniformly to the color range $0.6 < (B-V) < 0.9$. (*left*) The globular cluster feature of the spheroid luminosity function. The spheroid giant branch luminosity function is compared with the monotonic curve used in the first B&S paper (Bahcall & Soneira 1980). The need for the globular cluster feature is seen mainly from the analysis of star counts in the Basel fields SA 57 and SA 107.

to the end of hydrogen-burning main-sequence stars) and is equal to the observed value at $M_V = 12.5$. More recent observations all seem to suggest that the disk luminosity function decreases between absolute visual magnitudes 12.5 and 16 or 17, although the details in this important region are not yet certain (see the discussion in Section 3.9). The assumed disk luminosity function should be improved at the faint red end, although none of the comparisons considered in this review will be affected.

Upgren & Armandroff (1981) have stressed the significance of the difference between the smooth disk luminosity function determined by Luyten (1968) using his extensive proper-motion data and the luminosity function with a prominent dip that was obtained by Wielen (1974) from the Gliese (1969) catalog. Upgren & Armandroff argue that the completeness of the available samples supports the lower value for the disk luminosity function given by Wielen in the range of absolute visual magnitudes between +6 and +9. In the first discussion by Bahcall & Soneira (1980), an analytic disk luminosity function was used that represented the smooth Luyten (1968) function.

In order to calculate the distribution of disk stars in color as well as in apparent visual magnitude, we need to adopt a color-magnitude diagram for the model stars. We have used the data of Keenan (1963), Harris (1963), and Johnson (1965) for disk stars in the solar vicinity in order to construct a disk main sequence. The giant branch for the disk stars was assumed to be similar to M67 (Johnson & Sandage 1955). The fraction of stars on the main sequence in the plane of the disk is assumed (as a crude first approximation) to be given by Equation 1 of Bahcall & Soneira (1981a).

2.2.2 THE SPHEROID We assume that the spheroid field stars are roughly similar to the globular cluster stars, but we test observationally with the aid of the model which of the characteristics are shared and which are different. We compute models with and without a certain characteristic and search for observational domains that can distinguish between the different predictions. Thus we began in Paper I by assuming a spheroid luminosity function that was similar to the disk luminosity function (Equation 1 of Paper I) and have gradually improved this approximation in ways that are indicated by comparisons with data. *The approach we adopt is openly empirical, not theoretical. It is based upon comparing the model with observations, not upon deductions from stellar evolution theory.*

The luminosity function for the spheroid that is currently used in the Export Model is compared in Figure 12 with the assumed disk luminosity function. This figure is taken from Bahcall et al. (1985), in which both luminosity functions were described in detail. More accurate globular

cluster luminosity functions are being accumulated rapidly, and it will soon be necessary to replace the function shown in Figure 12 with a more modern version. At present, the differences between individual globular clusters are comparable to the difference between the adopted function shown in Figure 12 and the best luminosity function for any individual cluster. Under the circumstances, we prefer to maintain simplicity by using only the single simple function shown in the figure.

We have included the Wielen dip in the spheroid luminosity function as our standard option, although the model code permits one to make calculations with and without the dip. It will be of great interest to see whether both the disk and the spheroid populations contain this dip, a question that can only be answered by future observations.

The adopted spheroid luminosity function is cut off at $M_V = -3.0$ mag, since no globular cluster stars are observed brighter than this limit. It would be very interesting to test the assumption that the spheroid field stars, like the globular cluster stars, do not contain any young objects. Unfortunately, the number of predicted spheroid stars with $M_V < -3.0$ mag is too small to affect any of the calculations or comparisons with data that are discussed in the present review even if we used the original approximation that the luminosity function extends smoothly down to $M_V = -6.0$ mag.

The feature labeled "GCF"—globular cluster feature—is now included in the default luminosity function in the Export Code of the B&S Galaxy model (see, e.g., Bahcall & Ratnatunga 1985, Bahcall et al. 1985), although in previous versions of the code it was only an option (see Paper II). The data in three directions on the sky require (see Section 3.4) that the GCF be present in the luminosity function of spheroid field stars as well as of globular cluster stars (see, e.g., Da Costa 1982).

The color-magnitude diagram of the spheroid is important for observations in two or more colors that refer to intermediate apparent magnitudes (e.g. $15 < m_B, m_V < 19$). We show in Figure 13 the color-magnitude diagrams that we have used for illustrative purposes in the Export Code. The correct spheroid color-magnitude diagram probably has contributions from a number of different components or metallicities (see, for example, the excellent review by Kraft 1983). We have chosen the color-magnitude diagrams of the globular clusters M92 and 47 Tuc as examples of the extreme range of known Population II color-magnitude diagrams with very different metallicities; they have, respectively, [Fe/H] $\simeq -2.1$ and $\simeq -0.6$ (see Harris & Racine 1979, Zinn 1980). We also use the color-magnitude diagram of M13, with [Fe/H] $\simeq -1.4$ (Harris & Racine 1979), since it provides a good fit to much of the high-latitude data.

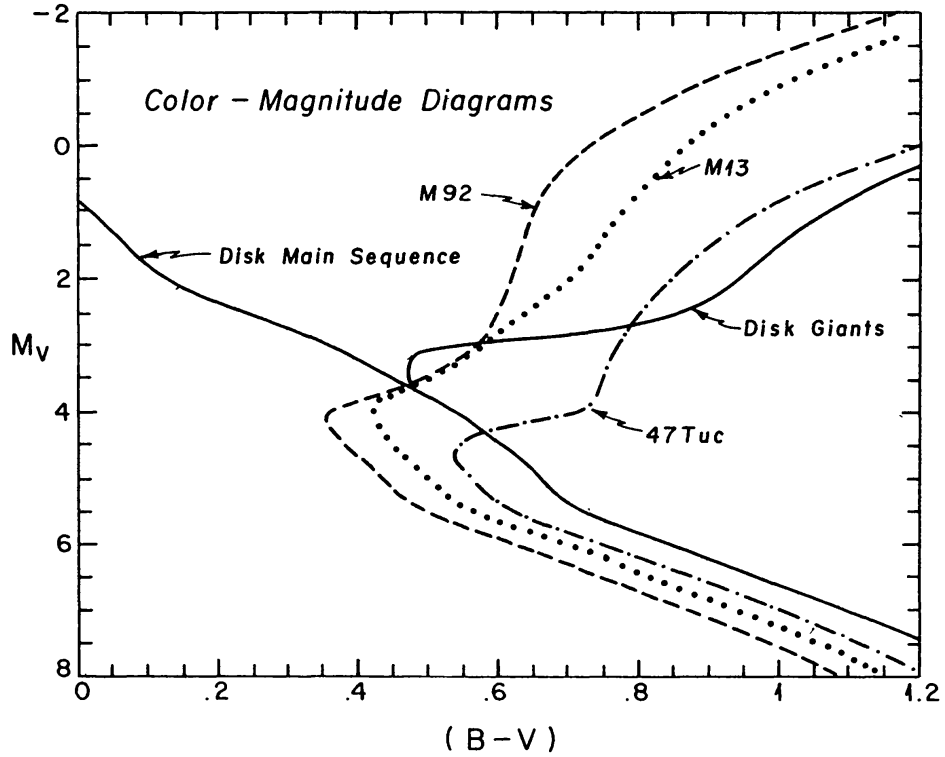

Figure 13 The color-magnitude diagrams. The color-magnitude diagrams for M13, M92, and 47 Tuc, taken from Sandage (1970, 1982), Hesser & Hartwick (1977), and Lee (1977). The disk color-magnitude diagram is shown for comparison. It was constructed from main-sequence data given by Johnson (1965, 1966) and Keenan (1963), with the giant branch assumed to be the same as that given by Morgan & Eggleton (1978) for M67.

2.3 *Scale Lengths and Scale Heights*

There are many determinations in the literature of the local scale heights of disk stars (see references in the caption of Figure 2 of Paper I). In accordance with this information, the older main-sequence stars (with $M_V > +5.1$) are assumed in the B&S model to have an exponential scale height of 325 pc, and the younger main-sequence stars (with $M_V < +2.3$) are taken to have a scale height of 90 pc. The scale heights are denoted by $H(M_V)$ in Table 1. For M_V between +2.3 and +5.1, the scale height is linearly interpolated between 90 and 325 pc (see Figure 2 of Paper I). We assume that the disk giants have an average scale height of 250 pc and that the white dwarfs have the same scale height as the old stars. The observational constraints on the scale heights that have been provided by comparisons of star counts with the predicted model distributions are described in Section 3.7 (and in more detail in Paper II).

The scale length of the spheroid that is implied by the density law

given in Table 1 was adopted following de Vaucouleurs (1977) and de Vaucouleurs & Buta (1978). We use a value of 8 kpc for the distance of the Sun from the center of the Galaxy. The results we have obtained so far are not sensitive to the precise values of the solar position or to the linear scale factors for the spheroid because the density functions are normalized in the solar neighborhood.

On the other hand, the predicted star distributions are sensitive (see Section 3.2) to the normalization at the Sun (in stars per cubic parsec) of the spheroid density and to the spheroid luminosity function (over a limited magnitude range; see Section 3.3). For relatively bright stars, e.g. $m_V < 19$, the predicted color distributions and star counts are also sensitive to the color-magnitude diagram of the giant branch of the spheroid stars [see Bahcall et al. (1983b) and Paper III]. Therefore, we can use star counts as a function of color and apparent magnitude to determine the spheroid normalization and to set constraints on the luminosity function and the color-magnitude diagram.

3. APPLICATIONS

We must first decide how accurate are the available data before making inferences based upon comparisons between the model predictions and the observations. I prefer to be conservative in estimating the errors in order to minimize the chances that theoretical inferences will later have to be retracted.

Systematic uncertainties are expected to be large compared with statistical errors, especially for the colors. Examples of possible systematic uncertainties include errors in calibration magnitudes, uncertainties in the wavelength sensitivity of the bands used, incompletely specified transformation equations (the relation between colors in two broadband systems may depend upon population), incompleteness of the sample, and contamination by galaxies. There are well-known examples in the literature in which significant systematic errors have been found in apparent magnitude scales and in color differences of stars within the magnitude range in which we are interested (see, e.g., Stebbins et al. 1950, Faber et al. 1976). In order to be able to decide which theoretical models fit the data satisfactorily, we must make some estimate of the likely uncertainties in the existing data.

The best way to estimate the systematic uncertainties is to compare the results obtained by different observers using independent techniques. Unfortunately, there are only a few fields in which the same observational parameters have been determined by different observers. Bahcall & Soneira

(1984) discussed three illustrative cases for which multiple observations are available. In addition, Koo & Kron (1982) have made a comparison of their data in SA 68 with those of Jarvis & Tyson (1981). As a rough guide, based upon the comparisons cited above, I normally assume that the state-of-the-art published data permit shifts of up to 0.2 mag in the color of certain features and of order 25% in the number of stars in a given color bin. Based upon the comparison of total star counts made by different observers in the direction of the north galactic pole (see Figures 4*c* and 4*d* of Paper II), I usually require agreement with the total number of counts to an accuracy of better than 20%. In order to increase the margin of safety without greatly decreasing the information content of the observations, I normally restrict comparisons of color distributions and star counts to one magnitude brighter than the quoted observational limits.

3.1 *The Spheroid Axis Ratio*

The axis ratio of the spheroidal star distribution can be determined (Papers I and II) by comparing the number of spheroid stars that are observed in different fields that lie in the plane perpendicular to the vector directed from the Sun to the galactic center (i.e. in the $l = 90°$, $270°$ plane). The number of spheroid stars with a given magnitude or color will be independent of galactic latitude in this plane if the spheroid is perfectly round (neglecting obscuration, which is appropriate for the case that is considered below).

The best available data for this purpose have been obtained by Kron (1978, 1980) and Koo & Kron (1982) for SA 57 and SA 68. The observations were made in the broad J and F bands. The star counts are of high quality in a two-magnitude range that is approximately centered on $m_V = 21$ mag.

The key to the analysis is that spheroid stars can be separated from disk stars in a frequency-color histogram for stars in certain magnitudes and directions. A double-peaked star distribution is predicted by the two-component Galaxy model (see Figure 8*c* of Paper I or Figure 3 of this paper) for a limited magnitude and color range that just happens to include the Kron data. Nearly all the model stars bluer than $J-F = 1.35$ mag are predicted to be spheroid stars, and nearly all the model stars redder than $J-F = 1.6$ mag are disk stars. The analysis was performed in both $B-V$ (Paper I) and $J-F$ (Paper II). A number of observational and theoretical uncertainties were considered, including using a variety of color-magnitude diagrams for the spheroid stars, taking into account the possibility of color shifts as large as 0.2 mag, assuming different amounts of reddening to SA 68, and including or omitting the Wielen dip in the spheroid lumi-

nosity function. The best fit to the Kron data corresponds (Paper II) to an axis ratio of 0.80, with a rather large uncertainty:

$$\frac{b}{a} = 0.80^{+0.20}_{-0.05}. \quad 2.$$

This result should be checked and improved by making observations in other fields that are sensitive to the spheroid axis ratio [see Bahcall & Soneira (1981b) for some suggested directions].

The result given in Equation 2 is in good agreement with the determination by Oort & Plaut (1975), who found $0.8 \leq b/a \leq 1.0$ for RR Lyrae variables in fields near the galactic center. Fall (1981) measured the axial ratio at galactocentric radii of about 2 kpc and found $b/a \simeq 0.8$ [see Figure 1 of Fall (1981) for the beautiful picture of the galactic bulge taken by R. E. Royer]. The result we obtain from star counts (Equation 1 above) refers to galactocentric distances of about 10 kpc, whereas the Oort & Plaut and the Fall determinations refer to much smaller distances. We conclude that there is no evidence for a large gradient in the axial ratio of the spheroid stars between 2 and 10 kpc. Frenk & White (1982) have reached similar conclusions for the globular cluster system, for which they find that $b/a \simeq 0.85 \pm 0.13$ (see also the earlier discussions referenced in the Frenk & White paper, but compare Zinn 1985).

3.2 *The Spheroid Normalization*

The separation of spheroid and disk stars in the frequency-color diagram permits one to determine the normalization of the spheroid density function by fitting the model results to the absolute number of observed stars. This determination of the spheroid density is of special interest because, unlike most other estimates of the spheroid normalization, the value obtained from star counts is *independent of kinematic assumptions* about the spheroid field population.

The number of spheroid stars between $M_V = 4$ and $M_V = 8$ at the solar position can be calculated from the best fit to the Kron data in either SA 57 or SA 68. One finds, using the form of the spheroid density law given in Table 1, that (Papers I and II)

$$n(4 \leq M_V \leq 8 \text{ mag}) = 2.65 \times 10^{-5} \text{ pc}^{-3}. \quad 3.$$

The uncertainty in this normalization is at least as large as 25% with the available data. The total number of spheroid stars at the solar position can be estimated by integrating the luminosity function shown in Figure 1 using the density normalization given in Equation 2. We find that

$$n(M_V \leq 16.5 \text{ mag}) \simeq 3 \times 10^{-4} \text{ pc}^{-3}. \quad 4.$$

Stars outside the observationally accessible range could contribute a larger number density [see, e.g., Paper III (especially Section 4) for some examples of models in which this uncertainty is evaluated].

The total mass and luminosity of the spheroid have been estimated in Paper III by using various assumptions about the spheroid luminosity functions outside the observed region. The results are $M_{\text{spheroid}}(\leq 16.5\, M_V) \approx (0.9\text{–}3.2) \times 10^9\, M_\odot$ and $-16.9 \geq M_{V,\,\text{spheroid}} \geq -19.0$.

Table 2 Comparison of model parameters: Bahcall-Soneira and Gilmore

Parameter	B&S (1980)	B&S (1984)	Gilmore (1984)
Solar Galactocentric Distance	8 kpc	8 kpc	9 kpc
DISK			
Scale Length	3.5 ± 0.5 kpc	3.5 kpc	4.0 kpc
Scale Height (Old Stars)	325 pc	325 pc	325 pc
Disk Luminosity Functions	Wielen (no dip)	Wielen (dip)	Wielen (dip)
Color Magnitude Diagram	M67	M67	Chiu (1980)
SPHEROID			
Local Normalization (to disk)	0.00125	0.002	0.00125
Density Law	de Vaucouleurs (also Hubble)	de Vaucouleurs	de Vaucouleurs
Minor/Major Axis	0.85	$0.80^{+0.20}_{-0.05}$	0.80
Effective Radius	2.7 kpc	2.7 kpc	3.0 kpc
Luminosity Function	Analytic	Globular Cluster	Figure 6 of Gilmore 1984
THICK DISK			
Local Normalization	—	—	0.02
Exponential Scale Height	—	—	1.3 kpc
Exponential Scale Length	—	—	4.0 kpc
Luminosity Function	—	—	Figure 6 of Gilmore 1984
Color Magnitude Diagram	—	—	47 Tuc

The spheroid normalization given in Equations 3 and 4 is about 1/500 times the number density of disk stars locally.

3.3 *The Slope of the Spheroid Luminosity Function*

The slope of the spheroid luminosity function can be determined (Papers I and III) in a region in which the spheroid dominates the differential star counts by comparing the observed number of stars per unit of magnitude with that predicted by the model. For certain magnitude ranges and directions that are indicated by the model, the slope of the spheroid luminosity function can be read off directly from the observed differential star counts.

This procedure has only yielded one number so far: the slope of the spheroid luminosity function in the absolute visual magnitude range between +4 and +8. Suppose that the spheroid luminosity function has the form $\Phi(M_V) \propto 10^{\gamma M_V}$; it then follows (Paper I) that $\gamma_{\text{eff}} = 0.145 \pm 0.035(1\sigma)$. Further determinations of the spheroid luminosity by star counts and colors should be made using the techniques described in Paper III. In particular, fields in different directions should be used to determine if the slope of the spheroid luminosity function depends in a measurable fashion upon position in the Galaxy.

3.4 *The Globular Cluster Feature*

The globular cluster feature (labeled GCF in Figure 12) is seen clearly in the luminosity function of several globular clusters (Da Costa 1982) near $M_V = +1$ to $+4$. The observations of the Basel group of SA 57 (at the north galactic pole) and SA 107 ($l = 6°$, $b = +41°$) provide the most sensitive tests for the existence of this feature in the luminosity function of the spheroid field stars.

Figure 11 (taken from Bahcall et al. 1985) compares the observed and calculated color distributions for stars in SA 107 that have G magnitudes in the range $16.4 < G < 18.3$ and $R < 17.2$. The agreement between the observations and the calculated model distributions is good if the GCF is included. On the other hand, if the GCF is omitted, a large unobserved peak is predicted near $G-R = 1.2$ mag. The inferred presence of the GCF is independent of the assumed spheroid color-magnitude diagram (Bahcall et al. 1985). The model calculations shown in the upper diagrams in Figure 11 were obtained using a 47 Tuc (metal-rich) color-magnitude diagram; the distributions shown in the bottom diagrams in Figure 11 were obtained using an M92 (metal-poor) color-magnitude diagram. Similar results were obtained using the color-magnitude diagrams of M3 and M13.

The observations in the direction of SA 57 (see Bahcall et al. 1985) and in the direction of the Morton-Tritton field (see Bahcall & Ratnatunga

1985) also require that the GCF be present in the luminosity function of the spheroid field stars. This result was expected by Gilmore (1983).

3.5 *Absence of the Blue Tip of the Horizontal Branch*

A surprising result of the comparison of the Galaxy model with observations has been the conclusion that the blue tip of the horizontal branch is greatly depleted for spheroid field stars (Bahcall et al 1983b; and Paper II, especially Table 5). The expected number of blue stars was calculated by assuming that the spheroid field population is represented by the luminosity function and color-magnitude diagram of each of the classical globular clusters M3, M13, and M92. There are an order-of-magnitude fewer spheroid field stars with $B-V < 0.2$ mag than are present proportionately in the three classical clusters listed above. The observations are consistent with the spheroid field stars having a stubby horizontal branch similar to what is seen in 47 Tuc (cf. Hesser & Hartwick 1977, Lee 1977).

3.6 *The Wielen Dip in the Disk Luminosity Function*

The Wielen dip in the disk luminosity function near $M_V = 7$ mag is a characteristic feature of the stars in the local neighborhood. It is of great interest to know if this feature is present in the luminosity function of disk stars at other positions in the Galaxy [see the discussion of Pritchet 1983].

This question has been answered for the field SA 51, which is almost exactly at the anticenter and is at a relatively low galactic latitude ($b = 21°$). The upper diagrams in Figure 10 compare the observed star counts (by I. King; see Chiu 1980) with the calculated counts using separately the Wielen (1974) and the Luyten (1968) luminosity functions. Recall from Section 2 that the Luyten luminosity function is smooth and does not show the Wielen dip. The theoretical and observational results are in excellent agreement when the Wielen luminosity function is used. The agreement is less satisfactory, especially at fainter magnitudes, when the Luyten function is used.

The necessity for including the Wielen dip is shown even more clearly when one considers the color distributions. The color distribution observed by King for stars brighter than apparent visual magnitude 19.5 is compared in the bottom diagrams in Figure 10 with the distributions calculated using the Wielen and the Luyten luminosity functions. The observed color distribution shows clearly that the Wielen function—with the dip near $M_V = 7$ mag, or $B-V \simeq 1$—is indicated by the data. This result is significant, since it shows that the Wielen feature is present in the luminosity function of disk stars that are at a characteristic distance of 0.6 kpc (according to the B&S Galaxy model).

3.7 *Scale Heights, Density Fluctuations, and Scale Lengths*

We can separate disk and spheroid stars by using the bimodal color distribution that appears at intermediate apparent magnitudes. Once the disk stars are isolated, we can then put observational constraints on scale heights, volume fluctuations, and the scale length. The results cited here are derived in Paper II.

Three fields (SA 57, SA 68, and SA 141) that have been extensively studied show a clear separation in color between disk and spheroid stars. In addition, SA 51 (which is in the anticenter direction) has a relatively unimportant spheroid contamination in the magnitude range for which observations are available. By comparing model predictions obtained using different values of the assumed disk scale heights with observations in each of the fields mentioned above, one obtained the following $1-\sigma$ limit on the scale heights of main-sequence disk stars: $H_{\rm disk} = 350 \pm 50$ pc, $5 \leq M_V \leq 13.5$ mag. A similar argument shows that the fluctuations in the volume density of disk stars are not large in the four directions considered, namely $n_{\rm disk}/n_{\rm solar\ vicinity} = 1.0 \pm 0.15$, $5 \leq M_V \leq 13.5$.

The disk giants are expected to be prominent only at apparent visual magnitudes brighter than 10. McLaughlin (1983) has assembled data in this magnitude range, and an analysis of his results yields $H_{\rm disk} = 250 \pm 100$ pc, $-1 \leq M_V \leq 3$ mag.

One can set a lower limit on the value of the exponential scale length h of the observed star density in the plane of the disk (cf. Table 1). This scale length cannot be so small that, contrary to observations, the disk densities that are inferred by comparison with observations in the direction of the galactic center and the anticenter are very different. The quantitative constraint implied by existing observations is 2.5 kpc $\leq h$ (Paper II).

3.8 *A Thick Disk?*

Does the Galaxy have a thick disk?

Yes, of course. In some improved approximation, the Galaxy must have many components (both for the disk and the spheroid). Some of these will stick up well above the younger disk components. (In fact, the thin disk has an exponential tail that extends far above the main disk.) We have already embodied this knowledge to a limited extent in the assumed dependence of scale height upon absolute magnitude that was discussed in Section 2.3 (see also Table 1). In order for the question to have quantitative meaning, one must test whether or not a specific model for a thick disk is necessary for describing the data and whether or not it offers a better improvement than other possible generalizations.

Gilmore & Reid (1983) proposed a specific model: a thick disk with a characteristic scale height that is about 1.5 kpc and that contains approximately 2% of the stars in the solar neighborhood. Gilmore & Reid concluded that the stellar population associated with their proposed thick disk is not the same as the Population II that was defined, for example, by Schmidt (1975), because the local number density of thick-disk stars is almost an order of magnitude larger than was estimated for Population II stars by other authors (e.g. Schmidt 1975, Paper I).

The original argument used to justify the addition of the Gilmore-Reid thick disk is incorrect. An examination of the argument shows how important it is to compare models and observations in the space of the observational parameters, without the introduction of additional assumptions. Gilmore & Reid (1983) used photometric parallaxes, assuming that all of the stars were on the main sequence. They argued that the B&S Galaxy model could not fit their observations, which were interpreted using main-sequence photometric parallaxes. However, they made the comparison of their observations with the B&S model in the theoretical plane of *absolute magnitudes* (see Figure 8 of Gilmore & Reid 1983). The assumption that all of the stars were on the main sequence was criticized by Bahcall & Soneira (see especially Section 10 of Paper II), who pointed out that most of the spheroid stars in the magnitude range studied by Gilmore & Reid were expected to be giants—and not dwarfs—according to the model. The Gilmore-Reid observations are well fit by the standard B&S model (see Figure 9 of this paper, Section 7a and Figures 13–14 of Paper II, and Bahcall & Ratnatunga 1985).

Gilmore & Reid (1983) derived the scale height of their thick disk by fitting with two exponentials the observed distribution of the number of stars versus apparent magnitude (or height above the plane). This argument is also misleading, since the predictions of the two-component (thin disk plus spheroid) B&S Galaxy model can be fit equally well by two exponentials [compare Figure 6 of Gilmore & Reid (1983) with Figure 24 of Paper II].

The parameters of a thick disk must be chosen carefully in order to avoid filling up the valley at $B-V \simeq +1$ between the two peaks, due to the thin disk and the spheroid, in faint-star counts (see Figure 7 and Table 5 of Paper III and Pritchet 1983). The original Gilmore & Reid (1983) parameters (1.5 kpc, 2.5% normalization relative to the thin disk) were in conflict with observations (see Figure 17 of Paper II) if a disk luminosity function was used for the thick-disk component.

More recently, Gilmore (1984) has proposed a Galaxy model that is similar to the Bahcall & Soneira (1980) model except for the addition of a thick disk with a spheroid-like luminosity function. The assumed

luminosity function does not contribute many stars near $B-V=1$. This suggested thick disk has no unique implications for star counts that would allow it to be isolated easily from the prominent thin disk and spheroid.

Table 2 (see p. 599) lists the parameters of the 1984 Gilmore model and compares the B&S and Gilmore models. Table 2 makes clear that the Gilmore model must yield results that are very close to the B&S model, since the differences in parameters are minor except for the thick disk, which has no unique and obvious observational characteristics (for star counts).

Bahcall et al. (1985) have verified quantitatively the similarity of the two models for the 17 fields shown in Figure 1. Given the assumption by Gilmore (1984) that the thick disk has a spheroid luminosity function, the thick disk contribution is not separable from the Bahcall-Soneira spheroid in any of the fields that were considered. Most recently, Friel & Cudworth (1986) have shown that a thick disk with the 2% normalization advocated by Gilmore (1984) is in conflict with their observations in the direction of Serpens, although a normalization of less than 1% could not be ruled out.

3.9 *The Faint End of the Disk Luminosity Function*

A study of the dynamics of stars perpendicular to the galactic disk shows that about 0.1 $M_\odot$ pc^{-3} of material has not yet been observed (Bahcall 1984, Oort 1960). It is possible that this unseen mass could be in the form of stars of mass $\leq 0.1\ M_\odot$; such stars would not be detected without special programs in the red or near-infrared. In order to account for the missing mass, the luminosity function would have to increase as $\Phi \propto 10^{\gamma M}$, where for absolute visual magnitudes we have $\gamma \simeq 0.01$ to 0.05, the value depending somewhat upon the mass-luminosity relation for these faint stars. The expected number of faint red disk stars can be calculated, for the luminosity function given above, using the Galaxy model.

Several observers have suggested that the luminosity function turns over below about $M_V = 13$ mag (see, for example, Schmidt 1983, Gilmore & Reid 1983, Gilmore et al. 1985, Boeshaar & Tyson 1985, and references therein). To strengthen these results, the photographic (or CCD) colors should be calibrated in terms of absolute magnitude and the sensitivity of the conclusions to the kinematic selection effects in proper-motion samples. Both of these effects will be studied more extensively over the next few years.

Of course, even if the luminosity function turns over in a range accessible to optical observers, the unseen mass could all be contained in stars too faint to burn hydrogen. A two-hump distribution, with a second peak somewhere in the range $0.01 \leq M \leq 0.08\ M_\odot$ might best be studied by infrared surveys such as were obtained by *IRAS*.

3.10 *Massive Unseen Halo*

Rotation curves measured for our Galaxy (Gunn et al. 1979) and almost all other observed galaxies are flat or slightly increasing out to $\gtrsim 30$ kpc; these curves require the existence of a massive halo component in most galaxies that has an approximate r^{-2} dependence over some range. All attempts to detect the light distribution from the postulated r^{-2} components have failed, which implies that the luminosity function for the halo is very different from that of the disk or spheroid components. There can be only a very small number of relatively bright stars ($M_V \lesssim +8$ or $\sim 0.5 M_\odot$) because these contribute significantly to the luminosity density. Hence, halo stars are expected to be intrinsically faint and red.

In order to predict how the halo may show up in the star counts, we need both a mass model of the Galaxy in order to estimate the local halo density in the solar neighborhood and a model for the observed stellar content. The rotation curve for *only* the disk and spheroid components falls monotonically beyond about 8 kpc (see Figure 11 of Paper I) and has a maximum rotation velocity of 170 km s^{-1}. However, the observed rotation curve for our Galaxy is approximately constant at 225 km s^{-1} from 4 kpc to at least 25 kpc (Gunn et al. 1979). To bring the model rotation curve into agreement with the observations, we must add a third component to the model Galaxy—a massive halo with a density that behaves like r^{-2} over some range—and a local normalization of 0.010 $M_\odot$ pc^{-3} (7% of the total density in the solar neighborhood). The resulting rotation curve is also shown in Figure 11 of Paper I. Using the stellar mass-luminosity relation, we can transform the mass densities into number densities and calculate the resulting star counts by assuming a luminosity function. The final results of our analysis are not very sensitive to the detailed shape of the halo density law nor even to the local halo mass density.

In order to set limits on the halo luminosity function, we first assume (Paper I) that there are no stars in the halo brighter than absolute magnitude M_0. (Otherwise their total surface brightness and star counts would have already been detected.) Then, for a worst-case analysis, we assume that all the halo stars have this maximum brightness M_0. Using the mass-luminosity relation for main-sequence stars, we obtain the number density of the halo stars. For apparent magnitudes m such that $10\,\text{kpc} \lesssim 10^{0.2(m-M_0+5)}$, the observed halo stars are relatively close by and are not affected by the shallow density gradient in the halo. Hence, the halo density is effectively constant, and the halo counts will increase approximately like $10^{0.6m}$.

The star counts at the north galactic pole are in excellent agreement

with the B&S Galaxy model without a massive halo to $m_V = 22$, the current observational limit (see Figure 2). There is no evidence in the available data for the rapid increase of the counts like $10^{+0.6m}$, which is the signature of stars from a massive halo.

The maximum brightness limit for the halo stars derived in Paper I is $M_0 = +14$. This is the brightest absolute magnitude that does not significantly affect the star counts or colors brighter than $m_V = 22$ mag. Stars of this absolute magnitude have a mass of 0.14 $M_\odot$ and a mass-to-light ratio in the visual band of 650 solar units. Hence, we have

$$(M/L)_{\text{halo stars}} \geq 650 \text{ solar units.} \qquad 5.$$

If the objects that make up the massive halo burn hydrogen [$M_0 \leq 16.5$ mag (mass $\geq 0.085\ M_\odot$)], then they will be detectable by observations that could be carried out with available techniques. Detailed calculations are presented in Bahcall & Soneira (1981b). Observations in the infrared I band to $m_I = 22$ should reveal the stellar components of a massive halo if the stars are anywhere on the hydrogen-burning main sequence. Stars that burn hydrogen have a mass-to-light ratio in the visual band of up to 4×10^3 solar units. If the massive halo is composed of stars that have not yet reached the main sequence, then the visual band mass-to-light ratio is greater than 10^9 solar units, and thus these stars will not be detectable by ordinary techniques.

3.11 *Sample Definition and Field Contamination*

The Galaxy model can be used to help plan observations. For many systematic programs, it is useful to have an a priori estimate of the number of stars of a particular type (luminosity class, color, or population) that are present in specified directions and in given apparent magnitude ranges. This information can easily be obtained from the Export Version of the B&S Galaxy model. For example, suppose you wanted to identify a sample of distant disk K dwarfs (in order to determine K_z). You could run the Export Version of the Galaxy model to calculate the expected number of candidate stars in the field of interest as a function of color and of apparent magnitude. With this information, you could then choose the color range of the sample to maximize the ratio of K dwarfs to other stars; in addition, you could select the size of the field to be studied so that it would give you approximately the desired number of sample stars.

The model can also be used to estimate the contamination of field galactic stars in a variety of observations. For example, if one is interested in the galaxy or quasar content of a specific field, in the globular cluster luminosity function around a distant galaxy, or in the color-magnitude diagram of galactic globular clusters, then one would like to have an

estimate for the likely contamination by galactic stars. The contamination of Oort's (1960) sample of disk K giants constitutes a different but interesting application of the B&S model. The model suggests (Bahcall 1984) that the existing samples of disk K giants are significantly contaminated by spheroid K giants beyond about 0.6 kpc. Very deep wide-field exposures represent another class of applications. It is useful to have a standard set of expected number densities (and color distributions) with which to compare the future deep exposures that will be obtained with ground-based or space telescopes. For the *Hubble Space Telescope* (HST), comparison between observed and expected stellar densities may show immediately whether or not an unexpected phenomenon has been detected by the HST cameras, which will have unprecedented ability to separate stars and galaxies at faint magnitudes.

As an initial guide in planning and interpreting a variety of observations, Ratnatunga & Bahcall (1985) have presented tables of the predicted foreground field star counts in the directions of 76 galactic globular clusters with $b > 10°$ and toward 16 Local Group galaxies.

3.12 *Surveys*

For any detector with a well-specified sensitivity, the fraction of stars in the Galaxy that are accessible to observation can be calculated from the model. This observable fraction is a universal function of the maximum distance from the Sun (R_{max}) at which a candidate object could still be detected. The observable fraction is tabulated in Table 1 of Bahcall & Piran (1983) for disk objects. The coverage of many high-energy astrophysics experiments (involving, for example, X-ray, gamma-ray, ultraviolet, infrared, neutrino, or gravitational-wave surveys) can be described in terms of this function.

4. NEXT THEORETICAL STEPS AND OPEN OBSERVATIONAL QUESTIONS

4.1 *Next Steps*

There are two obvious next steps in generalizing the galactic model described in this review: (*a*) include the galactic bulge, and (*b*) include kinematic motions.

The first generalization should be relatively simple, since one can assume as a first approximation that the density distribution of the bulge population has the form shown in Table 1. The shape of this density law is taken from Oort (1977) and is based upon the analysis of infrared data by Becklin & Neugebauer (1968), Oort (1971), and Sanders & Lowinger (1972). The mass distribution derived from this density law is consistent

with observations of the velocity dispersion and rotation velocity in the galactic center (see Paper I and Oort 1977). It should be relatively straightforward to include in the B&S model a luminosity function thought to be representative of the bulge of our Galaxy and of other similar galaxies and, together with the specified mass density, write a subroutine that predicts the total number of stars in directions near the galactic center. The trick will be to know how to take account of the effects of patchy obscuration and to find transformation equations from the $B-V$ colors in which the disk and spheroid star distributions are defined to the more appropriate far-red or infrared colors that are appropriate in studying the galactic center. If successful, this generalization should provide valuable insight into the nature of the bulge stars.

The second generalization—to include kinematics—is more difficult than it might seem. One needs to assume a distribution function in the three-space velocities for each of the populations (disk, spheroid, and bulge). The precise forms of these distribution functions are not specified by existing theories, but one may begin by assuming the approximate form of a Gaussian in three-space velocities. In principle, the distribution functions will depend (at least) upon absolute magnitude and position in the Galaxy. It will be necessary to proceed by making simple assumptions regarding these dependences, calculating the predicted stellar motions in different directions and magnitude ranges (and colors), comparing these calculations with existing catalogs of proper motions and of radial velocities, and iterating the results until a model is found that is consistent with all of the available data (which have been accumulated over several decades). Many surprises, as well as a much deeper insight into the nature of the Galaxy, will surely result from this generalization.

4.2 *Observational Questions*

I list in this section some of the more important questions that can be answered by future observations.

1. What is the shape of the disk luminosity function for stars less massive than 0.1 $M_{\odot}$ (see Section 3.9)?
2. What are the differences and similarities between the spheroid field population and the globular cluster stars (see Sections 3.3–3.5 and Kraft 1983)?
3. What are the more accurate values for the spheroid normalization and axis ratio (see Sections 3.1–3.2)?
4. Does the Wielen dip appear in the spheroid luminosity function (see Sections 2.2.2 and 3.6)? Does the spheroid luminosity function depend upon galactocentric position?

5. Is the spheroid density distribution best described by a de Vaucouleurs law, a Hubble law, or some other function?
6. What is the best overall approximation for the color-magnitude diagram of the spheroid field stars? Is the field color-magnitude diagram a linear combination of color-magnitude diagrams of well-known globular clusters (see Paper II)?
7. What properties of the stellar content of the Galaxy vary with galactocentric position (see Section 2)? For example, is there evidence for a metallicity gradient in the spheroid field stars (see Paper II)?
8. What are the shapes of the disk and spheroid luminosity functions at the bright (massive-star) end (see Section 2.2)?
9. Is the massive unseen halo of the Galaxy made up of faint stars (see Section 3.10)?
10. Does the Galaxy have a thick disk (see Section 3.8)?
11. Are the galactic bulge stars described by a simple model like that used here for the thin-disk and spheroid field stars (see Sections 2.1 and 4.1)?
12. What surprises will be revealed by the *Hubble Space Telescope* at faint magnitudes (see Papers I and II)?

ACKNOWLEDGMENTS

I am grateful to my collaborator and friend R. Soneira for years of fun and enlightenment associated with this work. This research was supported by the National Science Foundation Grants No. PHY-8217352 and NAS8-32902.

Literature Cited

Bahcall, J. N. 1984. *Ap. J.* 287: 926
Bahcall, J. N., Piran, T. 1983. *Ap. J. Lett.* 267: L77
Bahcall, J. N., Ratnatunga, K. U. 1985. *MNRAS* 213: 39
Bahcall, J. N., Ratnatunga, K. U., Buser, R., Fenkart, R. P., Spaenhauer, A. 1985. *Ap. J.* 299: 616
Bahcall, J. N., Schmidt, M., Soneira, R. M. 1983a. *Ap. J.* 265: 730 (Paper III)
Bahcall, J. N., Soneira, R. M. 1980. *Ap. J. Suppl.* 44: 73 (Paper I)
Bahcall, J. N., Soneira, R. M. 1981a. *Ap. J. Suppl.* 47: 357
Bahcall, J. N., Soneira, R. M. 1981b. *Ap. J.* 246: 122
Bahcall, J. N., Soneira, R. M. 1984. *Ap. J. Suppl.* 55: 67 (Paper II)
Bahcall, J. N., Soneira, R. M., Morton, D. C., Tritton, K. P. 1983b. *Ap. J.* 272: 627
Becker, W. 1965. *Z. Astrophys.* 62: 54
Becker, W. 1980. *Astron. Astrophys.* 87: 80
Becker, W., Steppe, H. 1977. *Astron. Astrophys. Suppl.* 28: 377
Becklin, E. E., Neugebauer, G. 1968. *Ap. J.* 151: 145
Boeshaar, P. C., Tyson, J. A. 1985. *Ap. J.* 90: 817
Bok, B. J. 1937. *The Distribution of Stars in Space*. Chicago: Univ. Chicago Press
Bok, B. J., Basinski, J. 1964. *Mount Stromlo Obs. Mem.* 4: 1
Burstein, D., Heiles, C. 1982. *Ap. J.* 87: 1165
Buser, R., Kaeser, U. 1983. In *The Nearby Stars and the Stellar Luminosity Function, IAU Colloq. No. 76*, ed. A. G. Davis Phillip, A. R. Upgren, p. 147. Schenectady, NY: L. Davis

Buser, R., Kaeser, U. 1985. *Astron. Astrophys.* 145: 1
Chiu, L. T. G. 1980. *Ap. J. Suppl.* 44: 41
Creze, M., Robin, A. 1986. *Astron. Astrophys.* In press
Da Costa, G. S. 1982. *Astron. J.* 87: 990
de Vaucouleurs, G. 1959. In *Handbuch der Physik*, ed. S. Flugge, 53: 311. Berlin: Springer-Verlag
de Vaucouleurs, G. 1977. *Astron. J.* 82: 456
de Vaucouleurs, G., Buta, R. J. 1978. *Astron. J.* 83: 1383
Faber, S. M., Burstein, D., Tinsley, B., King, I. R. 1976. *Astron. J.* 81: 45
Fall, S. M. 1981. In *The Structure and Evolution of Normal Galaxies*, ed. S. M. Fall, D. Lynden-Bell, p. 1. Cambridge: Cambridge Univ. Press
Fenkart, R. P. 1967. *Z. Astrophys.* 66: 390
Fenkart, R. P. 1968. *Z. Astrophys.* 68: 87
Fenkart, R. P. 1969. *Astron. Astrophys.* 3: 228
Fenkart, R. P., Schaltenbrand, R. 1977. *Astron. Astrophys. Suppl.* 27: 409
Fenkart, R. P., Wagner, R. 1975. *Astron. Astrophys.* 41: 315
Frenk, C. S., White, S. D. M. 1982. *MNRAS* 198: 173
Friel, E. D., Cudworth, K. M. 1986. *Astron. J.* 91: 293
Gilmore, G. 1983. In *The Nearby Stars and the Stellar Luminosity Function, IAU Colloq. No. 76*, ed. A. G. Davis Phillip, A. R. Upgren, p. 197. Schenectady, NY: L. Davis
Gilmore, G. 1984. *MNRAS* 207: 223
Gilmore, G., Reid, N. 1983. *MNRAS* 202: 1025
Gilmore, G., Reid, N., Hewett, P. 1985. *MNRAS* 213: 257
Gliese, W. 1969. *Veröff. Astron. Rechen-Inst., Heidelberg, No. 22*
Gunn, J. E., Knapp, G. R., Tremaine, S. D. 1979. *Astron. J.* 84: 1181
Harris, D. L. 1963. In *Basic Astronomical Data*, ed. K. Aa. Strand, p. 273. Chicago: Univ. Chicago Press
Harris, W. E., Racine, R. 1979. *Ann. Rev. Astron. Astrophys.* 17: 241
Hesser, J. E., Hartwick, F. D. A. 1977. *Ap. J. Suppl.* 33: 361
Hubble, E. 1930. *Ap. J.* 71: 231
Infante, L. 1986. Submitted for publication
Jarvis, J. F., Tyson, J. A. 1981. *Astron. J.* 86: 476
Johnson, H. L. 1965. *Ap. J.* 141: 170
Johnson, H. L. 1966. *Ann. Rev. Astron. Astrophys.* 4: 193
Johnson, H. L., Sandage, A. R. 1955. *Ap. J.* 121: 616
Kapteyn, J. C. 1922. *Ap. J.* 55: 302
Keenan, P. C. 1963. In *Basic Astronomical Data*, ed. K. Aa. Strand, p. 78. Chicago: Univ. Chicago Press
Koo, D. C., Kron, R. G. 1982. *Astron. Astrophys.* 105: 107
Kraft, R. P. 1983. In *Highlights of Astronomy*, ed. R. M. West, 6: 129
Kron, R. G. 1978. *Photometry of a complete sample of faint galaxies.* PhD thesis. Univ. Calif., Berkeley
Kron, R. G. 1980. *Ap. J. Suppl.* 43: 305
Lasker, B. M. 1985. In *Guide Star Selection System for ST Long-Term Activities, Symp. Astron From Measuring Machines*, ed. I. N. Reid, P. C. Hewett. In preparation
Lee, S. W. 1977. *Astron. Astrophys. Suppl.* 27: 381
Luyten, W. J. 1968. *MNRAS* 139: 221
McLaughlin, S. F. 1983. *Astron. J.* 88: 1633
Mihalas, D., Binney, J. 1981. *Galactic Astronomy: Structure and Kinematics.* San Francisco: Freeman. 331 pp.
Morgan, J. G., Eggleton, P. P. 1978. *MNRAS* 182: 219
Morton, D. C., Tritton, K. P. 1982. *MNRAS* 198: 669
Oort, J. H. 1938. *Bull. Astron. Inst. Neth.* 8: 233
Oort, J. H. 1960. *Bull. Astron. Inst. Neth.* 15: 45
Oort, J. H. 1971. *Pontif. Acad. Sci. Scr. Varia* 35: 321
Oort, J. H. 1977. *Ann. Rev. Astron. Astrophys.* 15: 295
Oort, J. H., Plaut, L. 1975. *Astron. Astrophys.* 41: 71
Peterson, B., Ellis, R., Kibblewhite, E., Bridgeland, M., Hooley, T., Horne, D. 1979. *Ap. J. Lett.* 233: L109
Pritchet, C. 1983. *Astron. J.* 84: 1476
Ratnatunga, K. U. 1983. *Outer regions of the galactic halo.* PhD thesis. Aust. Natl. Univ., Canberra
Ratnatunga, K. U., Bahcall, J. N. 1985. *Ap. J. Suppl.* 59: 63
Reid, G., Gilmore, G. 1982. *MNRAS* 201: 73
Rodgers, A. W., Harding, P., Ryan, S. 1986. Submitted for publication
Sandage, A. 1970. *Ap. J.* 162: 841
Sandage, A. 1972. *Ap. J.* 178: 1
Sandage, A. 1982. *Ap. J.* 252: 553
Sandage, A. 1983. *Proc. Conf. Kinematics, Dynamics and Structure of the Milky Way, Vancouver*, ed. W. H. Shuter, pp. 315–24. Dordrecht: Reidel
Sanders, R. H., Lowinger, T. 1972. *Astron. J.* 77: 292
Schaltenbrand, R. 1974. *Astron. Astrophys. Suppl.* 18: 27
Schmidt, M. 1975. *Ap. J.* 202: 22
Schmidt, M. 1983. In *The Nearby Stars and*

the Stellar Luminosity Function, IAU Colloq. No. 76, ed. A. G. Davis Phillip, A. R. Upgren, p. 155. Schenectady, NY: L. Davis
Seares, F. H. 1924. *Ap. J.* 59: 11
Seares, F. H., van Rhijn, P. J., Joyner, M. C., Richmond, M. L. 1925. *Ap. J.* 62: 320
Stebbins, J., Whitford, A. E., Johnson, H. L. 1950. *Ap. J.* 112: 469
Upgren, A. R., Armandroff, T. Z. 1981. *Astron. J.* 86: 1898
Weistrop, D. 1972. *Astron. J.* 77: 366
Wielen, R. 1974. In *Highlights of Astronomy*, ed. G. Contopoulos, 3: 395. Dordrecht: Reidel
Yilmaz, F. 1977. *Publ. Istanbul Obs. No. 98*
Young, P. A. 1976. *Astron. J.* 81: 807
Zinn, R. 1980. *Ap. J. Suppl.* 42: 19
Zinn, R. 1985. *Ap. J.* 293: 424